Ag-assisted lateral etching of Si nanowires and its application to nanowire transfer

Chuanbo Li,[1,a)] Kristel Fobelets,[2] Chang Liu,[2] Chunlai Xue,[1] Buwen Cheng,[1] and Qiming Wang[1]
[1]*State Key Laboratory on Integrated Optoelectronics, Institute of Semiconductors, Chinese Academy of Sciences, Beijing 100083, China*
[2]*Department of Electrical & Electronic Engineering, Imperial College London, Exhibition Road, London SW7 2AZ, United Kingdom*

(Received 23 August 2013; accepted 11 October 2013; published online 28 October 2013)

Ag-assisted anisotropic lateral etching along the ⟨100⟩ directions in Si nanowire arrays (Si NWAs) is investigated. It is found that Ag ions, generated by H_2O_2 oxidation of Ag particles, re-nucleate on the sidewalls of the nanowires, causing side etching and tapering of the wires. By enhancing the side etching effect, fractures can be formed at specific positions along the nanowires. This technique is applied to transfer large-area Si NWAs onto a glass substrate. © *2013 AIP Publishing LLC*. [http://dx.doi.org/10.1063/1.4826930]

Due to their unique one-dimensional physical morphology and associated electrical, mechanical, and thermal properties, silicon nanowires (NWs) are used in a multitude of applications, including nano-electronics, photonics, energy, and biosensors.[1–8] A variety of methods, such as chemical vapour deposition,[9,10] metal assisted chemical etching,[11–18] laser ablation,[19] and thermal evaporation,[20] have been developed to prepare high-quality NWs. Of these techniques, metal-assisted chemical etching[11–18] offers a simple and cheap way to prepare large-area arrays of long nanowires. The etching mechanisms have been widely investigated.[11–17] It is generally believed that the process proceeds as follows: electrons are exchanged between Si and an oxidizing agent, e.g., H_2O_2, catalyzed by Ag particles, forming SiO_2. Subsequently, the SiO_2 is removed by HF and the Ag particles sink further into the Si, creating Si NWs. The Ag particles help the top-down etching of Si along the ⟨100⟩ direction to form a Si nanowire array (Si NWA) .[12,13] Z. Huang *et al.* have discussed the influence of side etching in (111) Si substrates by controlling the concentration of H_2O_2[21] and O. J. Hildreth *et al.* found that the etching direction can be modified by adjusting the shape of catalysts.[22] Recently, reports appeared on lateral etching of Si NWAs for the formation of porous nanostructures along the side wall.[23–25] In this manuscript, we specifically investigate the influence of the density of nucleated Ag particles and its influence on the etch rate in different lattice orientations. The density of nucleated Ag particles is changed via thermal processes.

The proper use of side wall etching can help to control the etching process and design NWAs for specific applications. For example, for low cost, flexibility, low mass, biocompatibility, and optical transparency, it is preferable to have Si NWAs on support substrates such as metal foils, plastic sheets, and glass.[26–29] We investigate Ag-catalysed side etching and its impact on the formation of Si NWAs using a two-stage etching process. By using the side etching technique, large-area Si NWAs are transferred onto a glass substrate.

P-type Si (100) wafers with resistivity of 1–10 Ω·cm were used in our experiments. After cleaning with acetone, isopropanol and deionized (DI) water, the back side of the wafer was protected by sputter coated Cr/Au and spin-coated PMMA. In the 1st stage, the samples were immersed in a solution of 0.006 M silver nitrate ($AgNO_3$) and 5.6 M HF for 10–900 s, forming Ag particles on the surface. After rinsing in DI water, they were immediately transferred into a solution of 5.6 M HF and 0.3 M H_2O_2 for a 1 h 2nd stage etch to form Si NWs. After the 2nd stage, the sample was removed and soaked in a hot water bath at 80 °C for 3 h to loosen and redistribute the Ag particles at the bottom of the NWs. Finally, the sample is reloaded in the 2nd etch solution for a 3–6 min 3rd stage etch, that, due to lateral etching, forms cracks at the bottom of the NWs. The residual Ag particles were removed in a solution of highly concentrated HNO_3 (5 M). SEM and TEM are used to observe the morphology of the nanostructures.

Experimental results indicate that the density of Ag particles formed in the 1st stage plays an important role in the formation of the Si NWs (Figs. 1(a)–1(d)). In the case of a low Ag particle density, as shown in Fig. 1(a), porous Si forms (Fig. 1(c)) due to a lack of Ag nucleation sites.[30,31] Only when a very high density of Ag nano-particles covers the surface of the Si wafer (Fig. 1(b)) can the Ag-assisted 2nd stage etch form Si NWAs (Fig. 1(d)). The NW lengths can be controlled by etching time and their diameters have a wide distribution: 30–300 nm (insets Fig. 1(d)). This non-uniform diameter originates from the uneven Ag sizes and their random distribution on the Si surface. It is found that the NWs stand vertically and Si is etched down along the [001] direction.

Fig. 1(e) shows the Si NWAs at the edge of a (100) wafer. The numbers 100 and 010 in Fig. 1(e) indicate the [100] and [010] directions parallel to the Si (100) surface and 001 indicates the [001] direction perpendicular to the Si (100) surface. Clearly, the NWAs are oriented in three different perpendicular directions, demonstrating anisotropic etching

[a)]Author to whom correspondence should be addressed. Electronic mail: cbli@semi.ac.cn. Tel.:+86-10-82305061.

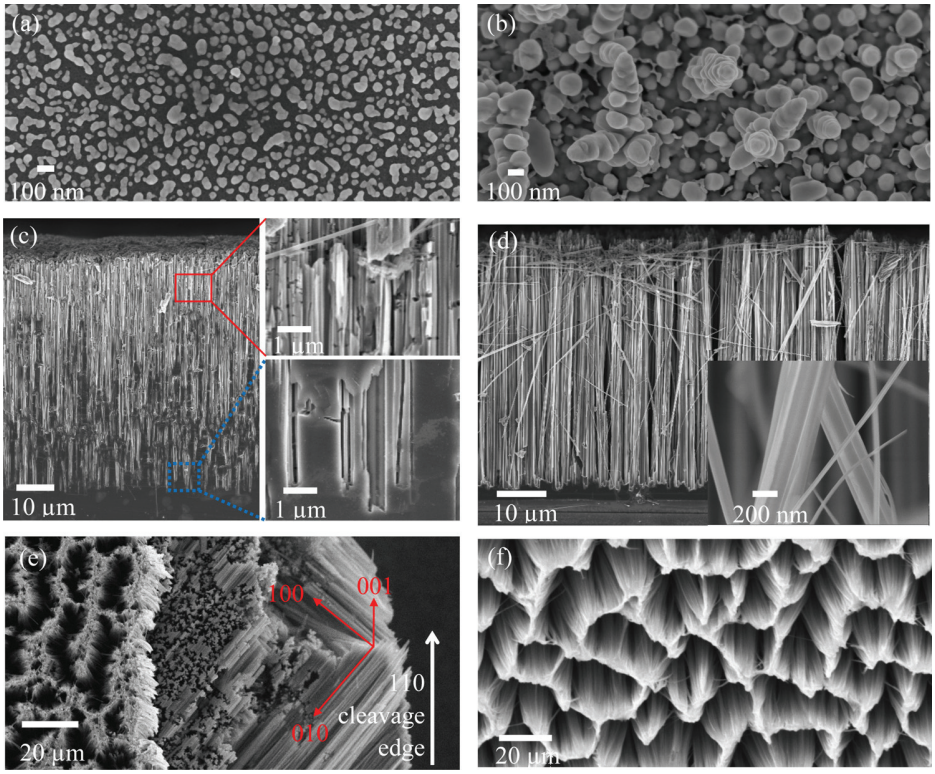

FIG. 1. SEM image of Ag particles for (a) 10 s and (b) 900 s 1st stage etch; (c) and (d) cross-section SEM of 2nd stage etch of (a) and (b), respectively. The insets show high magnification SEM images. Top-view of SEM images of the nanowire arrays at (e) the edge and (f) the middle of the sample.

along the [100], [010], and [001] directions. The etch rate in the three directions is approximately the same as deduced from the NW length. Compared to the typical [100] etch in the middle of the sample (Fig. 1(f)), the Ag particles nucleated on the (010) and (001) surfaces at the edge of the sample contribute to the side etching and formation of Si NWAs along [010] and [001]. This simultaneous 3-D etching removes the top part of the NWs at the edge (Fig 1(e)). Due to the water-based etching, the tops of the NWs structures agglomerate to form congregated bundles in order to reduce surface tension (Fig. 1(f)). These bundles can be removed by various processes.[31]

While the diameter of the NWs at the top is small, much wider buttressed structures are observed at the bottom of NWAs as shown in Figs. 2(a) and 2(b). We postulate that the buttressed structures arise from side etching in the middle of the wafer. In our etch process, Ag catalysts nucleate on the surface in the 1st stage and Si NWs are etched in the 2nd stage while no further Ag catalyst is supplied. In a control experiment, a Si sample is left for 3 h in the 2nd stage solution, no etching occurs when the Ag catalyst is absent. Thus, Ag-assisted chemical etching must contribute to the tapering of the NWs. It has been reported that Ag nanoparticles can be oxidized by H_2O_2 into Ag ions during the 2nd stage

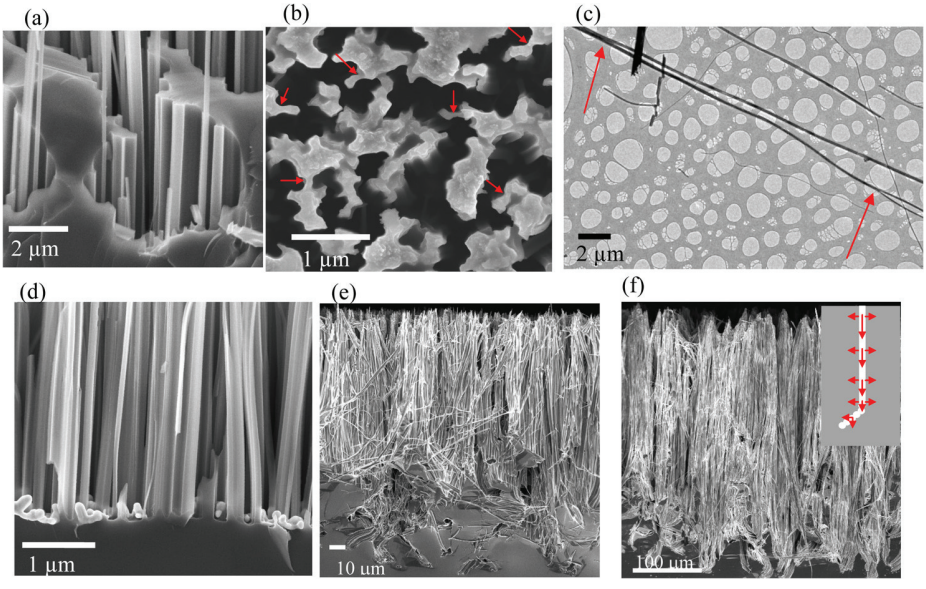

FIG. 2. (a) and(b) SEM images of the bottom of Si NWAs. (c) TEM image of a split Si NW. The arrows indicate the split points; (d) SEM image of the Ag catalysts at the bottom a Si NWA. SEM images of Si NW etched for 17 h with different Ag nucleation of (e) 10 min and (f) 30 min. Inset: schematic drawing of the etch rate variation from top to bottom.

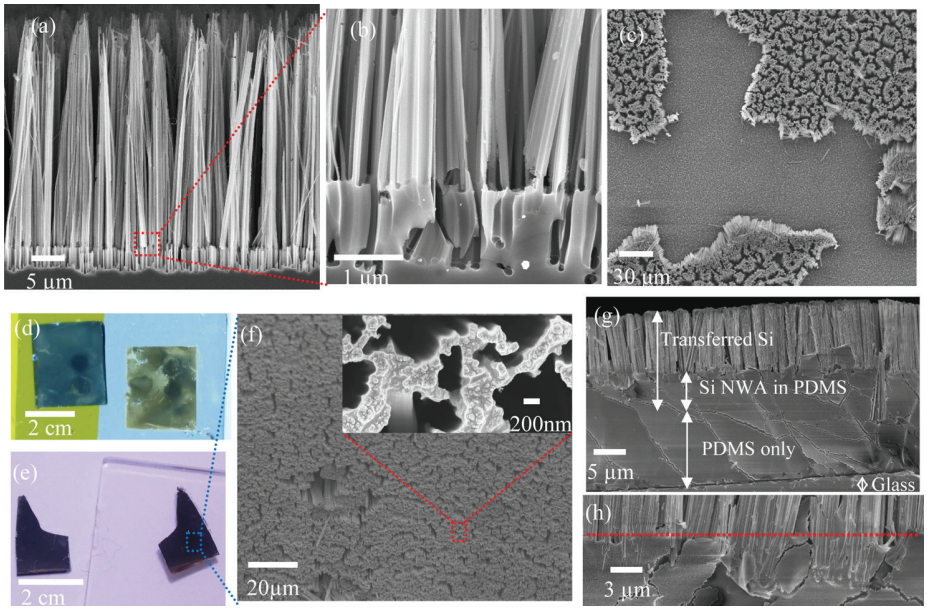

FIG. 3. (a) SEM image of the cracks at the bottom of a Si NWA and (b) at higher magnification. (c) Inhomogeneous NWA for a long 3rd stage etching step. (d, e) Optical images of transferred Si NWAs (right) and its residue substrate (left) on (d) a metal and (e) a glass substrate. (f) Top-view SEM image of the transferred Si NWAs onto glass. The inset shows a magnification. (g) Cross-section SEM image of transferred Si NWAs onto glass. (h) SEM image of the interface between PDMS and Si NWA, indicated by the dotted line.

etching process.[11,12] We suggest that the Ag ions in the solution re-nucleate on the sidewalls of the NWs and contribute to lateral etching. Our evidence to support this slow lateral etching process is that the buttressed structures can only be found at the bottom and not the top of the NWs in our experiments. This is also confirmed by TEM results shown in Fig. 2(c). The NW is split at the points indicated by the arrows. These splits are due to side etching, causing the division of one thick NW into three thinner ones. The longer the NWs remain in the etch solution, the higher the possibility for side etching. Thus, the buttressed structure is etched through the side at the thinner regions, as indicated by the arrows in Fig. 2(b), and forms separated thinner NWs. Compared to the fast top-down etching, the side etching rate in the middle of the wafer is slow since only tiny amounts of Ag particles re-nucleate on the sidewalls of the wires to assist this etching. Moreover, as the Ag particles formed in the 1st stage are partly consumed in the solution, due to H_2O_2 oxidization, the size of the Ag particles becomes smaller (Fig. 2(d)) compared to their original size (Fig. 1(a)). This is another contribution to the bigger NW size at the bottom of the NWAs. The case with a low density of nucleated Ag shows that the volume of etched material reduces with depth (see inset Fig. 1(c)). This is due to a competition between oxidizing Ag particles into the solution and re-nucleating particles on the sidewalls.

In a separate experiment, NWAs are etched for an extended time (17 h) with two different, but high concentrations of nucleated Ag. The samples underwent a 10 min and 30 min 1st stage nucleation time, respectively. It was found that the length of the vertical NWs is shorter ($\sim$119 μm versus $\sim$315 μm) when the available starting concentration of Ag is smaller. This is illustrated in Figs. 2(e) and 2(f). Once the main proportion of the initially available Ag particles concentration is consumed, side etching becomes important and the NWs are no longer mainly etched vertically. This experiment also confirms that the relative importance of side etching compared to down etching changes with available Ag concentration. At the end of the etch process, the rate of down etching and side etching becomes similar (see inset Fig. 2(f)).

Since the side etching is slow due to the small number of re-nucleated Ag, introducing a step to increase this density should increase the side etching rate. This can be done by removing the sample from the 2nd stage etch bath and soaking it in a hot water bath at 80 °C for 3 h.[26] Due to the large difference in thermal expansion coefficient between Ag and Si, the temperature changes help to loosen, break, and redistribute the Ag particles at the bottom of the NWs. Ag particles re-nucleate at any of the surrounding Si surfaces, thus also on the NW sidewalls. A 3–6 min 3rd stage etch causes lateral etching to form cracks at the bottom of the NWs (Figs. 3(a) and 3(b)). To prove the influence of thermal expansion, we have heated the samples in a dry environment on a hotplate at 150 °C for 1 min and found that Ag particles are also re-distributed as in the hot water bath and the cracks are properly formed in the 3rd stage etching. This forms vertically aligned Si NWAs with proper (4 min 3rd stage etching) cracks at the bottom which can be easily broken off from the Si bulk[27] and transferred onto, e.g., a glass substrate (Figs. 3(d) and 3(e)). We transferred NWAs into spin-coated Polydimethylsiloxane (PDMS) (sylgard®184) on glass. After spin coating, the PDMS is cured at 75 °C for 3 min on a hot plate. The Si NWA is pressed against the receiver substrate with a vertical pressure of 40 N/cm^2 to embed the NWAs into the polymer. Then PDMS is hardened at 160 °C for 5–10 min. Finally, the Si substrate is moved laterally in order to snap off the NWA in the PMDS by shear force and bending fracturing. The formation of proper cracks at the bottom of NWs and the adhesion strength between the NWs and polymer are key factors for NWA transfer. Cracks too far removed from the substrate—6 min 3rd stage etch—releases the NWAs with minimal agitation, leaving inhomogeneous NWAs (Fig. 3(c)). However, a too short 3rd stage etch hinders the breaking of the NWAs. In a control experiment, the transfer of Si NWAs without cracks is found to give poor

transfers. An irregularly shaped Si NWA sample demonstrates the transfer clearly. Fig. 3(e), right, is the transferred NWA pattern in PDMS on glass and Fig. 3(e), left, shows the identical shape of the residue substrate. Fig. 3(f) shows the top-view of the transferred Si NWAs and demonstrates the transfer of vertically oriented NWs. The top pattern of the transferred NWAs (inset of Fig. 3(f)) has a similar buttressed shape as those at the bottom of the NWAs shown in Fig. 2(b). From the cross-section SEM image (Figs. 3(g) and 3(h)), we find that the Si NWA is transferred onto glass with a 3–5 μm Si NW length inserted inside the PDMS. Reactive ion etching (RIE) of the transferred structure highlights the interface between PDMS and NWA. This is indicated by the dotted line in Fig. 3(h).

In conclusion, the density of the nucleated Ag particles formed in the 1st stage of a two-stage metal assisted electroless chemical NW etching process plays an important role in the formation of Si nanowires. When a high density of Ag particles is available from the 1st stage, the etching is mainly along the ⟨100⟩ directions. However, Ag particles re-nucleating during the etching process on the sidewalls of the NWs contribute to lateral etching of the nanowires. This lateral etching is slow compared to the down etching as long as the density of initially nucleated Ag particles is higher than the re-nucleated density. When the density of initial Ag particles drops to the same level as the re-nucleating particles, lateral etching becomes as important as vertical etching and etching of longer vertical NWs is impeded. By increasing the density of re-nucleating Ag particles, the side etching rate can be increased compared to the down etching rate. This can be used to under-etch the NWs to form cracks at the bottom of the NWs. Well positioned cracks can be used to transfer large-area Si NWAs onto alternative substrates.

This work was supported in part by the Major State Basic Research Development Program of China (Grant Nos. 2013CB632103 and 2011CBA00608), National Thousand Talents Program of China, the bilateral collaboration project between Chinese Academy of Sciences and Japan Society for the Promotion of Science (Grant No GJHZ1316), the National High-Technology Research and Development Program of China (Grant Nos. 2012AA012202 and 2011AA010302), the National Natural Science Foundation of China (Grant Nos. 61176013 and 61177038), and the *e-on* International Research Initiative project. C. Li thanks Z.A.K. Durrani for the discussion.

[1]H. J. Fan, P. Werner, and M. Zacharias, Small **2**, 700 (2006).
[2]J. Xiang, W. Lu, Y. J. Hu, Y. Wu, H. Yan, and C. M. Lieber, Nature **441**, 489 (2006).
[3]J. D. Holmes, K. P. Johnston, R. C. Doty, and B. A. Korgel, Science **287**, 1471 (2000).
[4]A. I. Hochbaum, R. Chen, R. D. Delgado, W. Liang, E. C. Garnett, M. Najarian, A. Majumdar, and D. Yang, Nature **451**, 163 (2008).
[5]B. Tian, X. Zheng, T. J. Kempa, Y. Fang, N. Yu, J. Huang, and C. M. Lieber, Nature **449**, 885 (2007).
[6]Y. Hwang, A. Bukai, and P. D. Yang, Nano. Lett. **9**, 410 (2009).
[7]Y. Cui, Q. Wei, H. Park, and C. M. Lieber, Science **293**, 1289 (2001).
[8]G. Zheng, F. Patolsky, Y. Cui, W. U. Wang, and C. M. Lieber, Nat. Biotechnol. **23**, 1294 (2005).
[9]F. Patolsky, B. P. Timko, G. Yu, Y. Fang, A. B. Greytak, G. Zheng, and C. M. Lieber, Science **313**, 1100 (2006).
[10]J. B. Hannon, S. Kodambaka, F. M. Ross, and R. M. Tromp, Nature **440**, 69 (2006).
[11]L. T. Canham, Appl. Phys. Lett. **57**, 1046 (1990).
[12]M. L. Zhang, K. Q. Peng, X. Fan, J. S. Jie, R. Q. Zhang, S. T. Lee, and N. B. Wong, J. Phys. Chem. C **112**, 4444 (2008).
[13]K. Q. Peng, A. J. Lu, R. Q. Zhang, and S. T. Lee, Adv. Funct. Mater. **18**, 3026–3035 (2008).
[14]Y. Q. Qu, L. Liao, Y. J. Li, H. Zhang, Y. Huang, and X. F. Duan, Nano Lett. **9**, 4539 (2009).
[15]Z. P. Huang, H. Fang, and J. Zhu, Adv. Mater. **19**, 744 (2007).
[16]K. Q. Peng, Y. Wu, H. Fang, X. Y. Zhang, Y. Xu, and J. Zhu, Angew. Chem., Int. Ed. **44**, 2737 (2005).
[17]K. Q. Peng, J. J. Hu, Y. J. Yan, Y. Wu, H. Fang, Y. Xu, S. T. Lee, and J. Zhu, Adv. Funct. Mater.**16**, 387 (2006).
[18]K. Q. Peng, Y. Xu, Y. Wu, Y. J. Yan, S. T. Lee, and J. Zhu, Small **1**, 1062 (2005).
[19]Y. F. Zhang, Y. H. Tang, N. Wang, D. P. Yu, C. S. Lee, I. Bello, and S. T. Lee, Appl. Phys. Lett. **72**, 1835 (1998).
[20]H. Pan, S. Lim, C. Poh, H. Sun, X. Wu, Y. Feng, and J. Lin, Nanotechnology **16**, 417 (2005).
[21]Z. Huang, T. Shimizu, S. Senz, Z. Zhang, N. Geyer, and U. Gosele, Phys. Chem. C **114**, 10683 (2010).
[22]O. J. Hildreth, W. Lin, and C. P. Wong, ACS Nano **3**, 4033 (2009).
[23]F. Bai, M. C. Li, D. D. Song, H. Yu, B. Jiang, and Y. F. Li, J. Solid State Chem.**196**, 596 (2012).
[24]W. McSweeney, O. Lotty, N. V. V. Mogili, C. Glynn, H. Geaney, D. Tanner, J. D. Holmes, and C. O'Dwyer, J. Appl. Phys. **114**, 034309 (2013);.
[25]X. P. Li, Y. J. Xiao, J. H. Bang, D. Lausch, S. Meyer, P. T. Miclea, J. Y. Jung, S. L. Schweizer, J. H. Lee, and R. B. Wehrspohn, Adv. Mater. **25**, 3187–3191 (2013).
[26]J. M. Weisse, D. R. Kim, C. H. Lee, and X. L. Zheng, Nano Lett. **11**, 1300 (2011).
[27]V. J. Logeeswaran, A. M. Katzenmeyer, and M. S. Islam, IEEE Trans. Electron Devices **57**, 1856–1864 (2010).
[28]J. M. Weisse, C. H. Lee, D. R. Kim, and X. L. Zheng, Nano Lett. **12**, 3339 (2012);.
[29]J. M. Weisse, C. H. Lee, D. R. Kim, L. L. Cai, P. M. Rao, and X. L. Zheng, Nano Lett. **13**, 4362–4368 (2013).
[30]Z. P. Huang, N. Geyer, P. Werner, J. de Boor, and U. Gösele, Adv. Mater. **23**, 285–308 (2011).
[31]C. B. Li, K. Fobelets, M. S. Tymieniecki, M. Hamayun, Z. A. K. Durrani, and M. Green, ECS Trans. **33**(38), 9–13 (2011).